

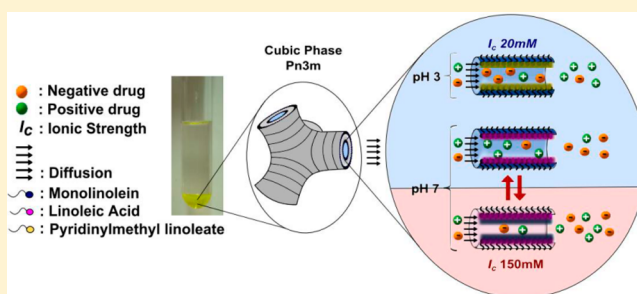
Influence of Electrostatic Interactions on the Release of Charged Molecules from Lipid Cubic Phases

Renata Negrini, Antoni Sánchez-Ferrer, and Raffaele Mezzenga*

ETH Zurich Food & Soft Materials Science, Institute of Food Nutrition & Health, Department of Health Science & Technology, Schmelzbergstrasse 9, LFO E23, 8092 Zürich, Switzerland

Supporting Information

ABSTRACT: The release of positive, negative, and neutral hydrophilic drugs from pH responsive bicontinuous cubic phases was investigated under varying conditions of electrostatic interactions. A weak acid, linoleic acid (LA), or a weak base, pyridinylmethyl linoleate (PML), were added to the neutral monolinolein (ML) in order to form lyotropic liquid-crystalline (LLC) phases, which are negatively charged at neutral pH and positively charged at acidic pH. Release studies at low ionic strength ($I = 20$ mM) and at different pH values (3 and 7) revealed that electrostatic attraction between a positive drug, proflavine (PF), and the negatively charged LLC at pH = 7 or between a negative drug, antraquinone 2-sulfonic acid sodium salt (AQ2S), and the positively charged LLC at pH = 3 did delay the release behavior, while electrostatic repulsion affects the transport properties only to some extent. Release profiles of a neutral drug, caffeine, were not affected by the surface charge type and density in the cubic LLCs. Moreover, the influence of ionic strength was also considered up to 150 mM, corresponding to a Debye length smaller than the LLC water channels radius, which showed that efficient screening of electrostatic attractions occurring within the LLC water domains results in an increased release rate. Four transport models were applied to fit the release data, providing an exhaustive, quantitative insight on the role of electrostatic interactions in transport properties from pH responsive bicontinuous cubic phases.



INTRODUCTION

Bicontinuous cubic phases formed by self-assembly of monoglycerides in water are viscous complex fluids with a well-defined inner structure consisting of a highly curved continuous lipid bilayer separating two interpenetrating aqueous channels.^{1–3} A well-known example of these systems is represented by the monolinolein–water system, which self-assembles into liquid-crystalline phases of various geometries at body temperature (37 °C).⁴ When water is added to the lipid monolinolein (ca. 35%), the bicontinuous cubic phase with crystallographic space group $Pn3m$ is formed, which retains the structure up to excess water conditions.⁵ Due to the unique structural features and the thermodynamic equilibrium in excess water conditions, such mesophase is highly promising in controlled drug delivery, being relevant in biology, chemistry, food science, pharmaceutical sciences, and medicine.^{6–9} It has been reported that the cubic $Pn3m$ phase formed by monoglycerides shows sustained release properties.^{10,11} However, these neutral systems alone are typically not capable of responding to important biological stimuli such as pH or ionic strength.

In the last years, stimuli responsive drug delivery systems have gained attention because of their ability to reduce toxicity and side effects associated with traditional release systems. One of the most widespread approaches consists of doping monoglyceride-based lyotropic liquid crystals (LLCs) with

different molecules to introduce responsive moieties.^{12–18} This approach mostly leads to two different scenarios: (i) adjustment of the structure during the application of the stimuli,^{19–22} or (ii) a controlled release due to specific interactions between the drug and the LLC environment.^{23–27} In the present work, we are concerned with the second strategy, and in particular with the effect of electrostatic interactions between the functional mesophases and model drugs.

Already back to 1998, Lindell et al. studied the effect of ionic strength changes in the transport properties of the bicontinuous cubic phases, where negatively charged phospholipids were added to neutral monoolein in order to tune the release of a positively charged drug timorol.²³ In this way, charges were screened and the drug molecule was released as if a neutral system was employed. Later on, in 2005, Caffrey and Clogston further demonstrated that the release of different drugs could be controlled by adjusting the nature and the degree of the interactions between the hosting cubic phase and the drug present in the aqueous medium.²⁴ To this end, oleic acid was added to the neutral monoolein system, and the release of the positive drug ruthenium-tris(2,2'-bipyridyl) dichloride was tuned by addition of salt. In both studies, the pH responsive

Received: March 3, 2014

Revised: March 27, 2014

Published: March 27, 2014

behavior was not assessed, and the mesophase changed during the releasing process.^{23,24} In 2011, Kwon and Kim reported an example of pH responsive bicontinuous cubic phase, where the pH response was obtained without changing the structure and where protonation and deprotonation of the carboxylic acid groups was used as a triggering mechanism.²⁵ This strategy was further exploited recently by Landau et al. to actuate a pH-controlled release of doxorubicin.²⁷ In all the above mentioned studies, attractive electrostatic interactions can be actuated solely in the presence of positively charged drugs and negatively charged mesophases. Recently, we have shown how a positively charged mesophases can also be used to control transfection of negatively charged biomacromolecules such as DNA, by using a monolinolein-based mesophase modified by an alkyl primary amine.²⁸ While this greatly increases the scope of responsive mesophases, electrostatic interactions remain difficult to be fully exploited by pH changes due to the strongly basic behavior of alkyl primary amines.

The present work introduces a new general concept for pH responsive bicontinuous cubic phases, which can be both negatively charged at neutral pH and positively charged at moderately acidic pH. The work builds on the previous studies about the role of electrostatic interactions on the drug release behavior of lipid mesophases, but goes beyond the state of the art by considering the most comprehensive set of interactions investigated to date, including attractive, repulsive, screened attractive, or neutral electrostatic interactions. All these conditions have been screened by exploiting the possibility of controlling the release at different pH in both positively and negatively charged drugs, and by doping the *Pn3m* bicontinuous cubic monolinolein system with either a weak acid or a weak base without changing the mesophase structure. Screened electrostatic interactions are studied by varying the ionic strength to values ($I = 20$ and 150 mM) at which the Debye length is either larger or smaller than the water channel radii, respectively. Finally, we rationalize the release properties at varying electrostatic conditions by comparing the fit to diffusion curves from four different diffusion models, which allows extracting the main essential features ruling the diffusion under changing electrostatic interactions.

MATERIALS AND METHODS

Materials. Dimodan U/J (Danisco, Denmark, batch no. 015312) was used as received. This commercial-grade form of monolinolein (ML) contains more than 98 wt % monoglyceride. Linoleic acid (LA), caffeine, proflavine (PF), anthraquinone 2-sulfonic acid sodium salt (AQ2S), ethanol, the necessary compounds for the different buffers (4-(2-hydroxyethyl)-1-piperazineethanesulfonic acid (HEPES), sodium chloride, hydrochloric acid, sodium hydroxide, phosphoric acid), and 4-pyridinemethanol, 4-dimethylaminopyridine, *N,N'*-dicyclohexylcarbodiimide, dichloromethane, and *n*-hexane were purchased from Sigma-Aldrich-Chemie (Schnelldorf, Germany). Milli-Q water was used for all the experiments. Pyridin-4-ylmethyl linoleate (PML) was synthesized and characterized with different techniques as detailed in the Supporting Information.

Preparation and Loading of the Lyotropic Liquid-Crystalline Phases. Proflavine (PF), anthraquinone 2-sulfonic acid sodium salt (AQ2S), and caffeine were dissolved in buffer solutions (pH 3 and 7) at 0.1, 0.1, and 0.5 wt % respectively. The pH was measured and the solutions were kept in the dark to avoid any drug photodegradation prior to mixing them with the lipids. For all the experiments at low ionic strength ($I = 20$ mM) and physiological conditions ($I = 150$ mM), phosphate buffer for pH = 3 and HEPES buffer for pH = 7, were used, respectively. In order to form the lipid phases with 0.5 wt % linoleic acid (LA) or with 2 wt % pyridinylmethyl linoleate (PML),

9.95 g of ML and 0.05 g of LA or 9.8 g of ML and 0.2 g of PML respectively, were weighed and mixed in ethanol. The solvent was then evaporated and the mixtures were dried under vacuum. Samples of drug-loaded LC phases were prepared by weighing the appropriate amount of the lipid mixture (0.195 g) and different buffers (0.105 g) into Pirex tubes, where the aqueous solution comprised 35 wt % of the total mesophase. The lipidic and aqueous materials were mixed by heating and vortexing in a cyclic way. The LLC bulk phases were then equilibrated in the oven at 37 °C for 24 h and covered with aluminum foil in order to avoid photodegradation of the drug. At the end of the equilibration, each LLC mesophase was sampled for the characterization of the mesophase by X-ray diffraction.

Release Studies. For the release studies, a precise amount of buffer at the chosen pH (3 or 7) and ionic strength ($I = 20$ or 150 mM) was added on top of the loaded and equilibrated *Pn3m* mesophases with a sufficient excess of buffer in a ratio mesophase/buffer of 1:9. In order to simulate perfect sink conditions, the buffer solution was then periodically replaced by an identical amount of fresh buffer, and the amount of drug released measured by means of UV-vis spectroscopy. At the end of each release experiment, the LC mesophase was characterized by small-angle X-ray diffraction to rule out potential structural changes during the study. All the release studies were done in triplicates.

Small Angle X-ray Scattering Measurements. SAXS measurements were used to identify the symmetry of the mesophases at the different conditions. Experiments were performed using a Rigaku MicroMax-002+ microfocussed beam X-ray source operating at 45 kV and 0.88 mA. The Ni-filtered Cu $K\alpha$ radiation ($\lambda_{Cu\ K\alpha} = 1.5418$ Å) was collimated by three pinhole collimators (0.4, 0.3, and 0.8 mm in diameter), and the data were collected by a two-dimensional argon-filled Triton-200 X-ray detector (20 cm diameter, 200 μ m resolution). An effective scattering-vector range of 0.03 Å⁻¹ < q < 0.45 Å⁻¹ was probed, where q is the scattering wave-vector defined as $q = 4\pi \sin \theta / \lambda_{Cu\ K\alpha}$ with a scattering angle of 2θ . For all measurements, the samples with a sample thickness of ca. 1 mm were placed inside a Linkam HFS91 stage, between two thin mica sheets and sealed by an O-ring. Measurements were performed at 37 °C, and samples were equilibrated for 30 min prior to measurements, while the scattered intensity was collected over 30 min.

UV-Vis Measurements. The amount of drug released at different times was measured by UV-Vis analysis using a Varian Cary 100 Bio UV/Vis spectrophotometer. Measurements were done at room temperature and for each drug a wavelength scan was performed to determine the suitable wavelength. In particular, $\lambda = 444$ nm for proflavine, $\lambda = 256$ nm for anthraquinone 2-sulfonic acid sodium salt, and $\lambda = 273$ nm for caffeine were chosen. For each molecule, a calibration curve was constructed at different pH, and the drug concentration in solution was obtained by interpolation from the corresponding calibration curve. The absorbance at the same wavelength for blank samples without drugs was also measured, showing no evidence of released impurities.

RESULTS AND DISCUSSION

Data Analysis. The release profiles have been fitted with four different empirical models to better describe the phenomena involved in the process. These models allowed for the calculation of parameters such as the apparent diffusion coefficient, the initial diffusion velocity, and the maximum amount of drug released at infinite time for the different systems and conditions.

Drug release from mesophases has been shown to be primarily controlled by diffusion,^{29,30} for this reason, the first model considered was the one based on the Higuchi model:³¹

$$\frac{M_t}{M_{in}} = \frac{M_0}{M_{in}} + (k_H t)^{0.5} \quad (1)$$

where M_t (mol), M_{in} (mol), and M_0 (mol) are the amount of the drug released at time t , inside the mesophase before starting the study, and released at time zero, respectively; k_H (h^{-1}) is the release rate constant which is related to the apparent diffusion coefficient D ($cm^2 h^{-1}$).

In order to discriminate between different release kinetics, the following more general power equation introduced by Ritger–Peppas³² was also considered:

$$\frac{M_t}{M_{in}} = \frac{M_0}{M_{in}} + (k_{RP}t)^n \quad (2)$$

where k_{RP} (h^{-1}) is the release rate constant incorporating structural and geometric characteristics of the system and n is the release exponent, which is indicative of the drug release mechanism. When the release exponent is 0.5, the diffusion controlled process dominates (Higuchi model), while values between 0.5 and 1 indicate the presence of the so-called “anomalous” transport with the corresponding overlapping of different types of transport phenomena.³²

The previous mentioned models are approximations of the solution for Fick's law, and are very useful for obtaining information about the apparent diffusion coefficient but they can be applied only in the linear regime of the release experiment (when the ratio $M_t/M_{in} < 60\%$). Consequently, some interesting information cannot be extracted, such as the maximum concentration reached at the end of the release process, which can be related to the amount of drug retained into the mesophase due to specific interactions. For this reason, two more models have been considered in this work: the Weibull and the Peleg model.

The stretched exponential growth model, introduced by Weibull³³ is expressed by the form:

$$\frac{M_t}{M_{in}} = \frac{M_0}{M_{in}} + A(1 - e^{-(k_W t)^B}) \quad (3)$$

where A is related to the increase in concentration at the equilibrium at infinite time, B is the stretching exponent and k_W (h^{-1}) is the release rate constant related to the apparent diffusion coefficient. It can be observed that this model is associated with the Higuchi model. In fact, for small values of $k_W t$ and by considering $A = 1$ and $B = 0.5$, the Higuchi model represents the first part of the linear Taylor expansion of the Weibull model. Thus, a deviation from the pure diffusive state can also be attributed by comparing the values of the stretching exponent obtained. On the other hand, the sigmoidal Peleg function³⁴ is extensively employed to study the absorption kinetic of water in food and polymers, while here has been used to characterize the release behavior. The model is expressed by the form:

$$\frac{M_t}{M_{in}} = \frac{M_0}{M_{in}} + \frac{t}{k_1 + k_2 t} \quad (4)$$

where k_1 (h) and k_2 (dimensionless) are the Peleg's first and second constants. The apparent diffusion coefficients D ($cm^2 h^{-1}$) have been calculated by means of the following equation:

$$D = k \left(\frac{V}{2A} \right)^2 \pi \quad (5)$$

where k is k_H , k_{RP} , k_W , or k_1^{-1} , V (cm^3) is the volume of the mesophase, and A (cm^2) is the surface area exposed to the release medium.

In any case, it should be kept in mind that these relatively simple mathematical equations can be used to quantitatively describe drug release from predominantly diffusion-controlled delivery systems, but the apparent diffusion coefficients determined with the presented models are somewhat disentangled from the real values; nonetheless, these models allow for the comparison of release behavior in different systems and different regimes, and give access by extrapolation to important parameters. In particular, the last two models are very useful for the evaluation of the equilibrium relative molar concentration (C_{max}) and, by difference, the calculation of the amount of drug retained in the mesophase. The following equations were employed for the calculation of C_{max} by both the Weibull and Peleg model:

$$C_{max,W} = \frac{M_0}{M_{in}} + A \quad (6)$$

$$C_{max,P} = \frac{M_0}{M_{in}} + \frac{1}{k_2} \quad (7)$$

Moreover, it is possible to calculate from the Peleg model the initial release velocity V_0 (h^{-1}) as follows:

$$V_0 = \frac{1}{k_1} \quad (8)$$

and subsequently correlate it with the apparent diffusion coefficient calculated from the other three models.

Effect of the Electrostatic Interactions: Release Studies at Different pH and Low Ionic Strength. Release experiments at low ionic strength ($I = 20$ mM) were performed to prove electrostatic interactions of positive and negative drugs, proflavine (PF) and antraquinone 2-sulfonic acid sodium salt (AQ2S), with the corresponding counter-charged pH responsive cubic LLC mesophase. Release profiles of a neutral drug, caffeine, were also measured as a reference system since this molecule is not affected by the surface charges in the cubic LLCs. In order to study all possible ionic interactions between the drug and the water channels surface, positive–negative, positive–positive, negative–positive, and negative–negative, two different pH values (3 and 7) were considered. To obtain mesophases negatively charged at neutral pH or positively charged at acidic pH, ML was loaded with 0.5 wt % of LA or with 2 wt % of PML, respectively. The geometry of the different mesophases was analyzed by SAXS before and after each release study in order to monitor possible structural changes. The results show that $Pn3m$ bicontinuous cubic phase, characterized by reflections spaced as $\sqrt{2}:\sqrt{3}:\sqrt{4}:\sqrt{6}:\sqrt{8}:\sqrt{9}$ was maintained, and the lattice parameter was not affected by the presence of charges on the lipid–water interface (see the Supporting Information). The SAXS curves for the mesophase loaded with linoleic acid (LA) at pH = 7 undergo a very moderate shift in the lattice parameter from 9.01 to 9.20 nm, which corresponds to a water channel diameter of 3.94 and 4.02 nm, respectively. This change in the dimensions might possibly be due to the presence of charges which can promote hydration which, however, does not significantly affect the release of the drug molecules. For the sake of comparison, each pH release study was performed in both doped and neutral LLCs. All the molecules selected for this work are shown in Figure 1.

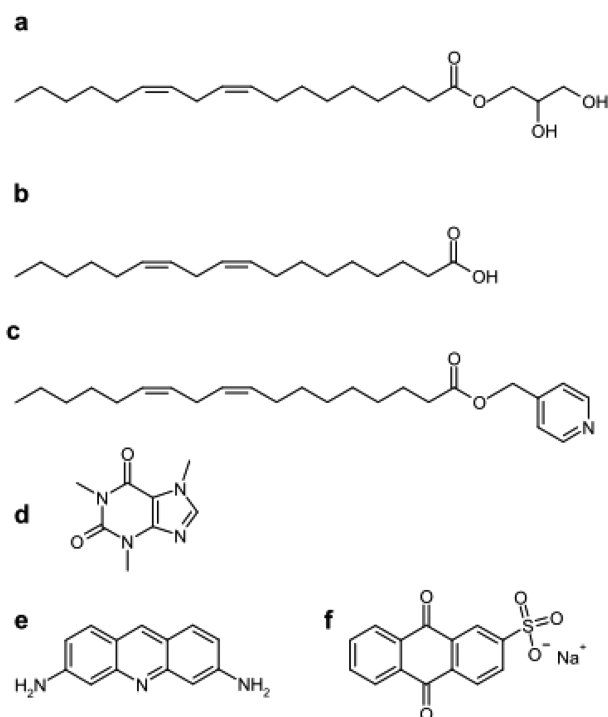


Figure 1. Chemical structures of (a) monolinolein (ML), (b) linoleic acid (LA), (c) pyridin-4-ylmethyl linoleate (PML), (d) caffeine, (e) proflavine (PF), and (f) anthraquinone 2-sulfonic acid sodium salt (AQ2S).

The release behavior of the three different drugs from the neutral mesophase at pH = 7, observed over 6 days at 37 °C, exhibited a sustained release mechanism (Figure 2).

From the logarithmic plot (Figure 2A) the exponential factor (n) has been evaluated by fitting the experimental data with the Ritger–Peppas model and compared with the Higuchi model in order to determine the mechanism involved in the process. The values obtained for the exponential factor were all above 0.5, proving that the release was not purely diffusive but specific interactions occurred between the drug and the mesophase. Likewise, the Weibull and the Peleg models have been used to fit the profiles of drug released as a function of time (Figure 2B). Again the stretched exponent values obtained from the Weibull model underline a deviation from the pure diffusive mechanism (see the Supporting Information). As it can be

seen, good agreement between theoretical values (solid lines) and experimental data (symbols) were obtained in all cases, as shown from the values of the correlation parameter R (Table 1). The apparent diffusion coefficients were calculated by using eq 5 and the corresponding values are reported in Table 1.

The release of caffeine resulted faster compared to the charged drugs; for instance, caffeine was completely released in 36 h instead of the only 60% of PF and AQ2S, probably because of its smaller size ($D_{\text{caffeine}} = 0.76 \text{ nm}$, $D_{\text{PF}} = 1.14 \text{ nm}$, $D_{\text{AQ2S}} = 1.11 \text{ nm}$) and its neutral charge which minimized specific interactions with the mesophase. Additionally, the maximum concentration evaluated by means of eqs 6 and 7 showed that all drugs were completely released (Table 1). This result demonstrated that, even if the system is not purely diffusive, all the drugs are completely released from the mesophase because no interactions occur in the absence of charged surface channels.

The influence of electrostatic interactions on the release behavior was first assessed by release studies of the positive drug, proflavine (PF), at two different pH values (3 and 7) for the doped (LA and PML) and the neutral systems (Figure 3).

Also in this case, the process was not purely diffusive (Figure 3A). The release profiles of the neutral system was faster at pH 3 compared to pH 7 due to the increase of the population of charged molecules when decreasing pH, which has a direct impact on the chemical potential driving force of the diffusion. An important decrease in the release rate was observed in the presence of linoleic acid (LA) at pH 7 (Figure 3B). The apparent diffusion coefficient for the LA doped system at pH 7 was estimated by means of the four different models: Higuchi, Ritger–Peppas, Weibull, and Peleg. The values obtained were, respectively, 3.7×10^{-4} , 5.4×10^{-4} , 21×10^{-4} , and $21 \times 10^{-4} \text{ cm}^2 \text{ h}^{-1}$. These values correspond to a decrease of 42%, 40%, 5%, and 36% for the doped system compared to the neutral one (Table 1). Consistently, the initial release velocity (V_0) calculated by using eq 8 was 35% smaller in the LA doped case. Moreover, the total concentrations obtained from the Weibull and the Peleg models (Figure 3B) indicate that 15% or more of the drug was retained when the LA loaded mesophase was deprotonated. This is attributed to the capacity of the LA charged headgroup to attract, and therefore retain the positive drug. This phenomenon was already reported by Lindell et al.²³ in the study above-mentioned, where the release data were normalized with the plateau end-points, considered as the

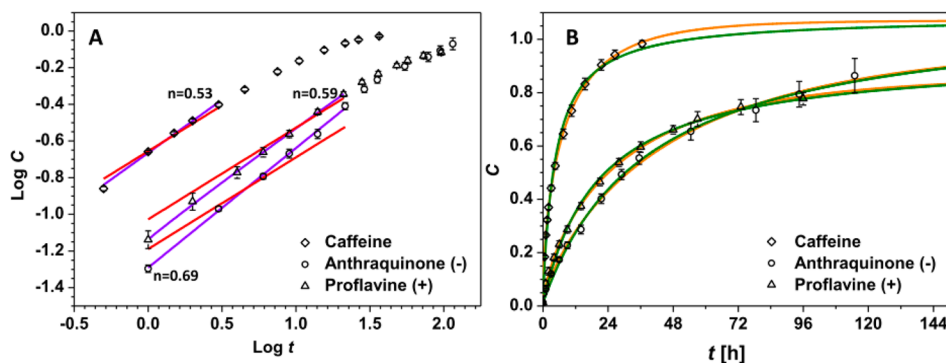


Figure 2. Release profiles of ML, the neutral bicontinuous cubic phase, at pH 7 and at 37 °C for the different drugs [(\diamond) caffeine, (Δ) proflavine, and (\circ) anthraquinone 2-sulfonic acid sodium salt]. (A) Log–log plot of the drug release process and the corresponding fitting curves for the Higuchi (red) and the Ritger–Peppas (violet) models. (B) Lin–lin plot of the drug release process and the corresponding fitting curves for the Weibull (orange) and Peleg (green) models. The data shown are the mean values \pm standard deviation.

Table 1. Fitting Parameters and the Corresponding Correlation Parameter R Obtained from the Higuchi, the Ritger–Peppas, the Weibull, and the Peleg Models: Apparent Diffusion Coefficient D ($\text{cm}^2 \text{h}^{-1}$), Maximum Release Concentration C_{max} (%), and Initial Velocity V_0 (h^{-1})

system/pH	Higuchi		Ritger–Peppas		Weibull		Peleg				
	D ($\text{cm}^2 \text{h}^{-1}$) ($\times 10^{-4}$)	R	D ($\text{cm}^2 \text{h}^{-1}$) ($\times 10^{-4}$)	R	D ($\text{cm}^2 \text{h}^{-1}$) ($\times 10^{-4}$)	C_{max}	R	D ($\text{cm}^2 \text{h}^{-1}$) ($\times 10^{-4}$)	C_{max}	V_0 (h^{-1}) ($\times 10^{-2}$)	R
P(+)/D/pH7	6.4 ± 0.3	0.98	9.0 ± 0.2	0.9991	22 ± 2	0.91 ± 0.03	0.9996	33 ± 2	0.93 ± 0.03	4.5 ± 0.2	0.998
P(+)/LA/pH7	3.7 ± 0.2	0.991	5.4 ± 0.3	0.9991	21 ± 3	0.72 ± 0.03	0.998	21 ± 2	0.81 ± 0.03	2.9 ± 0.2	0.996
P(+)/D/pH3	10.8 ± 0.3	0.98	12 ± 1	0.995	22 ± 2	1.11 ± 0.03	0.9997	46 ± 3	1.07 ± 0.03	6.3 ± 0.4	0.998
P(+)/PML/pH3	12.1 ± 0.3	0.990	13 ± 1	0.998	22 ± 1	1.14 ± 0.02	0.9998	52 ± 4	1.06 ± 0.03	7.1 ± 0.5	0.996
A(-)/D/pH3	4.9 ± 0.3	0.97	7.7 ± 0.4	0.997	21 ± 1	0.83 ± 0.01	0.9998	24 ± 1	0.94 ± 0.01	3.3 ± 0.1	0.9993
A(-)/PML/pH3	1.6 ± 0.1	0.95	3.7 ± 0.2	0.9994	14 ± 1	0.58 ± 0.01	0.9995	12 ± 1	0.65 ± 0.01	1.70 ± 0.05	0.9990
A(-)/D/pH7	4.7 ± 0.4	0.97	8.5 ± 0.3	0.997	15 ± 2	0.98 ± 0.05	0.9990	21 ± 1	1.11 ± 0.03	2.9 ± 0.1	0.9990
A(-)/LA/pH7	7.7 ± 0.4	0.97	10 ± 1	0.997	17 ± 1	1.07 ± 0.02	0.9998	32 ± 2	1.10 ± 0.03	4.4 ± 0.2	0.998
C(n)/D/pH7	37 ± 1	0.996	42 ± 3	0.998	82 ± 3	1.07 ± 0.01	0.99990	158 ± 10	1.04 ± 0.02	22 ± 1	0.995
C(n)/LA/pH7	36.1 ± 0.5	0.996	39 ± 2	0.998	66 ± 3	1.15 ± 0.02	0.99990	159 ± 12	1.02 ± 0.03	22 ± 1	0.995
P(+)/LA/pH7/150	6.1 ± 0.3	0.96	8.6 ± 0.3	0.995	22 ± 1	0.89 ± 0.02	0.9998	29 ± 1	0.97 ± 0.02	4.0 ± 0.2	0.9990

completed release of the “unbound” drug. In that work, the release drug concentration versus the square root of time was plotted (Higuchi model), and the slopes obtained were all in the same value range proving that the release mechanism and release rate were the same for the “unbound” fraction of drug, independently of the electrostatic interactions involved. In the present work, however, the diffusion coefficients have been calculated by taking in consideration the total amount of drug initially loaded in the mesophase. Thus, the diffusion coefficient from our results should therefore be taken as a global diffusion coefficient, averaged among both populations of “bound” and “unbound” drug molecules present in the system.

Electrostatic interactions between likewise charges were also studied and were found to affect only to some extent the diffusive process, thus the PML doped system at pH 3 behaved nearly like the neutral one. The apparent diffusion coefficients for the doped system at pH 3 were, respectively, 12.0×10^{-4} , 13.0×10^{-4} , 22×10^{-4} , and $52 \times 10^{-4} \text{ cm}^2 \text{ h}^{-1}$. These values correspond to an increase of 12%, 8.3%, 0%, and 13% of the PML doped system compared with the neutral one (Table 1). Moreover, the initial velocity (V_0) of the neutral system was 89% of that measured in the doped mesophase, and in both cases the entire drug was released (Table 1).

The same approach was applied to investigate the influence of the electrostatic interactions in the release behavior of the negative drug, anthraquinone 2-sulfonic acid sodium salt (AQ2S), at two different pH values (3 and 7) for the doped (LA and PML) and the neutral systems. To do so, the systems involved were exchanged: the PML doped system was employed to prove attractive interaction at pH 3, while the LA doped system was used to investigate repulsive interactions at pH 7 (Figure 4).

The presence of the pyridinylmethyl linoleate (PML) led to a decrease in the diffusion coefficients at pH 3. The values obtained were, respectively, 1.6×10^{-4} , 3.7×10^{-4} , 14×10^{-4} , and $12 \times 10^{-4} \text{ cm}^2 \text{ h}^{-1}$. These values correspond to a decrease of 67%, 52%, 30% and 50% in the apparent diffusion coefficient of the doped phase compared to the neutral one (Table 1). Consistently, the initial release velocity (V_0) calculated from the Peleg model was 49% smaller in the PML doped case than in the neutral system. Furthermore, the total concentrations obtained from the fitting (Figure 4B) indicate that nearly 30% of the drug was retained during the process due to charge interactions (Table 1). The electrostatic interactions between likewise charges slightly affected the diffusive process. The values obtained for the doped system at pH 7 were, respectively, 7.7×10^{-4} , 10×10^{-4} , 17×10^{-4} , and $32 \times 10^{-4} \text{ cm}^2 \text{ h}^{-1}$. The LA doped system was faster than the neutral one. This corresponds to an increase of 64%, 18%, 13%, and 52% of the LA doped system compare to the neutral one (Table 1). Moreover, the initial velocity (V_0) of the neutral system was 64% of the doped one, and in both cases all the drug was released (Table 1). In conclusion, the results obtained were in agreement with the previous one on the positive drug release; in both cases the presence of charged surfactants reduces the diffusivity because of the increase in the “bound” drug fraction, which diffuses at a slower rate compared to the “unbound” molecules. However, in this specific case repulsive interactions have a greater effect on the release behavior, leading to a noticeable increase in the diffusion rates.

Unperturbed Release: Neutral Drug Release. In order to underline the direct correlation between charge interactions among drug and water channels and the pH responsiveness of

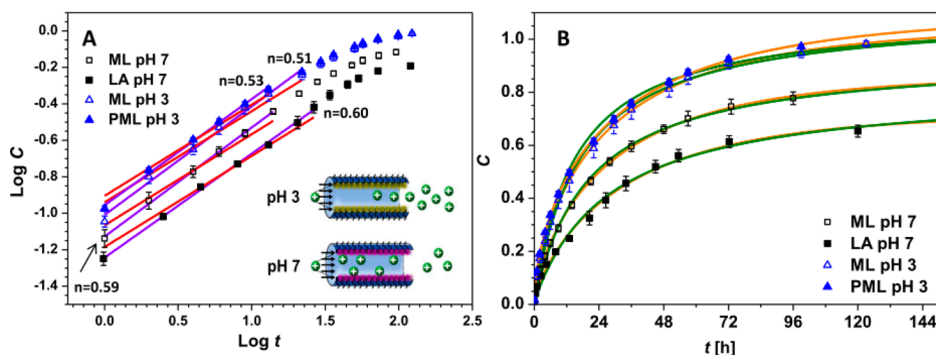


Figure 3. pH-induced changes in the release of the positively charged drug, proflavine (PF), from the pH responsive and neutral bicontinuous cubic phases at 37 °C. Release profiles of the drug from LA, the LA loaded mesophase (■), and ML, the relative neutral system (□), at pH 7, and from PML, the PML loaded mesophase (▲), and ML, the relative neutral system (△), at pH 3. (A) Log–log plot of the drug release process and the corresponding fitting curves for the Higuchi (red) and the Ritger–Peppas (violet) models. (B) Lin–lin plot of the drug release process and the corresponding fitting curves for the Weibull (orange) and Peleg (green) models. The data shown are the mean values \pm standard deviation.

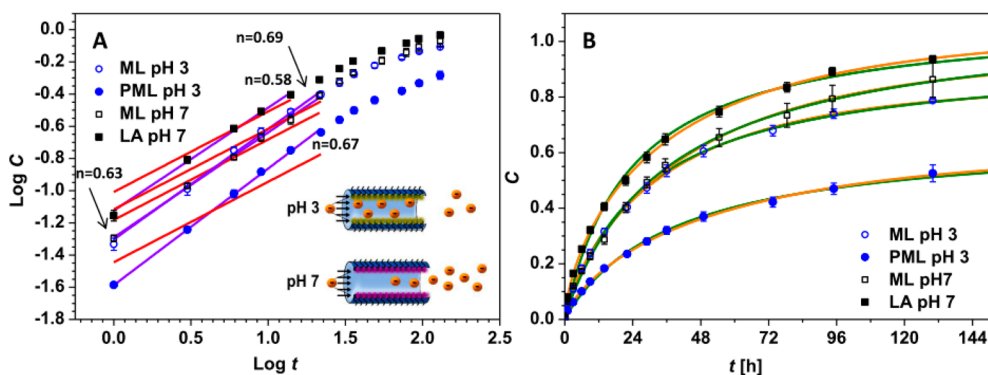


Figure 4. pH-induced changes in the release of the negatively charged drug—antraquinone 2-sulfonic acid sodium salt (AQ2S), from the pH responsive and neutral bicontinuous cubic phases at 37 °C. Release profiles of the drug from LA, the LA loaded mesophase (■), and ML, the relative neutral system (□), at pH 7, and from PML, the PML loaded mesophase (●), and ML, the relative neutral system (○), at pH 3. (A) Log–log plot of the drug release process and the corresponding fitting curves for the Higuchi (red) and the Ritger–Peppas (violet) models. (B) Lin–lin plot of the drug release process and the corresponding fitting curves for the Weibull (orange) and Peleg (green) models. The data shown are the mean values \pm standard deviation.

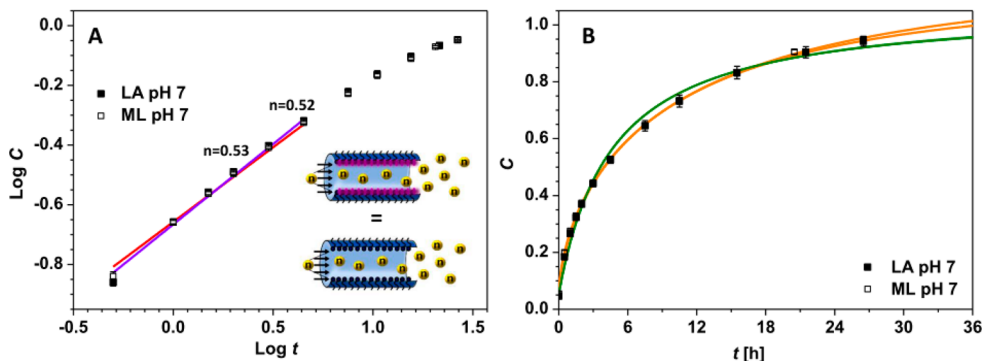


Figure 5. Release profiles of the neutral drug caffeine from LA, the LA loaded mesophase (■), and ML, the relative neutral system (□), at pH 7. (A) Log–log plot of the drug release process and the corresponding fitting curves for the Higuchi (red) and the Ritger–Peppas (violet) models. (B) Lin–lin plot of the drug release process and the corresponding fitting curves for the Weibull (orange) and Peleg (green) models. The data shown are the mean values \pm standard deviation.

the systems, release studies of the neutral drug caffeine were also measured and the profiles from charged and neutral mesophases compared (Figure 5).

As a proof of concept, LA loaded system at pH 7 was taken as example of charged system which can influence, by means of electrostatic interactions, the release behavior. The apparent diffusion coefficients were calculated and the respective values

in both cases were 36.1×10^{-4} , 39.0×10^{-4} , 66×10^{-4} , and $159 \times 10^{-4} \text{ cm}^2 \text{ h}^{-1}$ for the doped systems and 37.0×10^{-4} , 42.0×10^{-4} , 82×10^{-4} , and $158 \times 10^{-4} \text{ cm}^2 \text{ h}^{-1}$ for the neutral system proving that neutral drugs are released from charged and neutral mesophases in the same manner, as a result of lack of electrostatic interactions. The drug was entirely released (Table

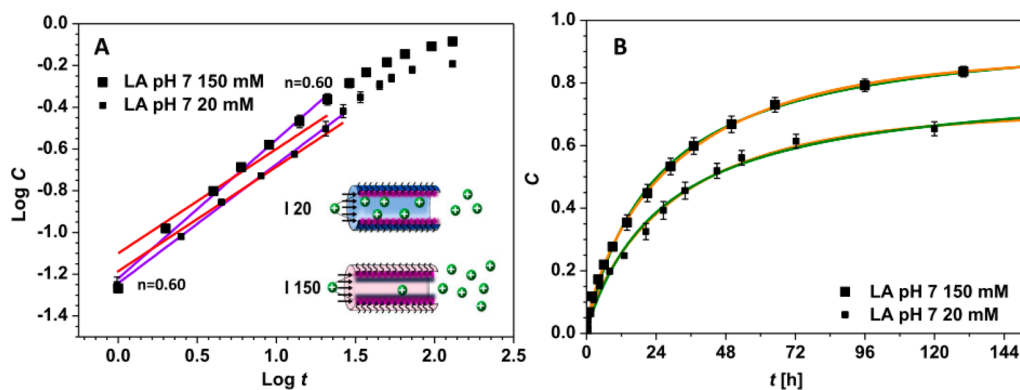


Figure 6. Effect of the ionic strength on the release behavior of the positively charge drug, proflavine (PF), from LA, the LA loaded mesophase (small ■) at $I = 20$ mM and $I = 150$ mM (large ■), at pH 7. (A) Log–log plot of the drug release process and the corresponding fitting curves for the Higuchi (red) and the Ritger–Peppas (violet) models. (B) Lin–lin plot of the drug release process and the corresponding fitting curves for the Weibull (orange) and Peleg (green) models. The data shown are the mean values \pm standard deviation.

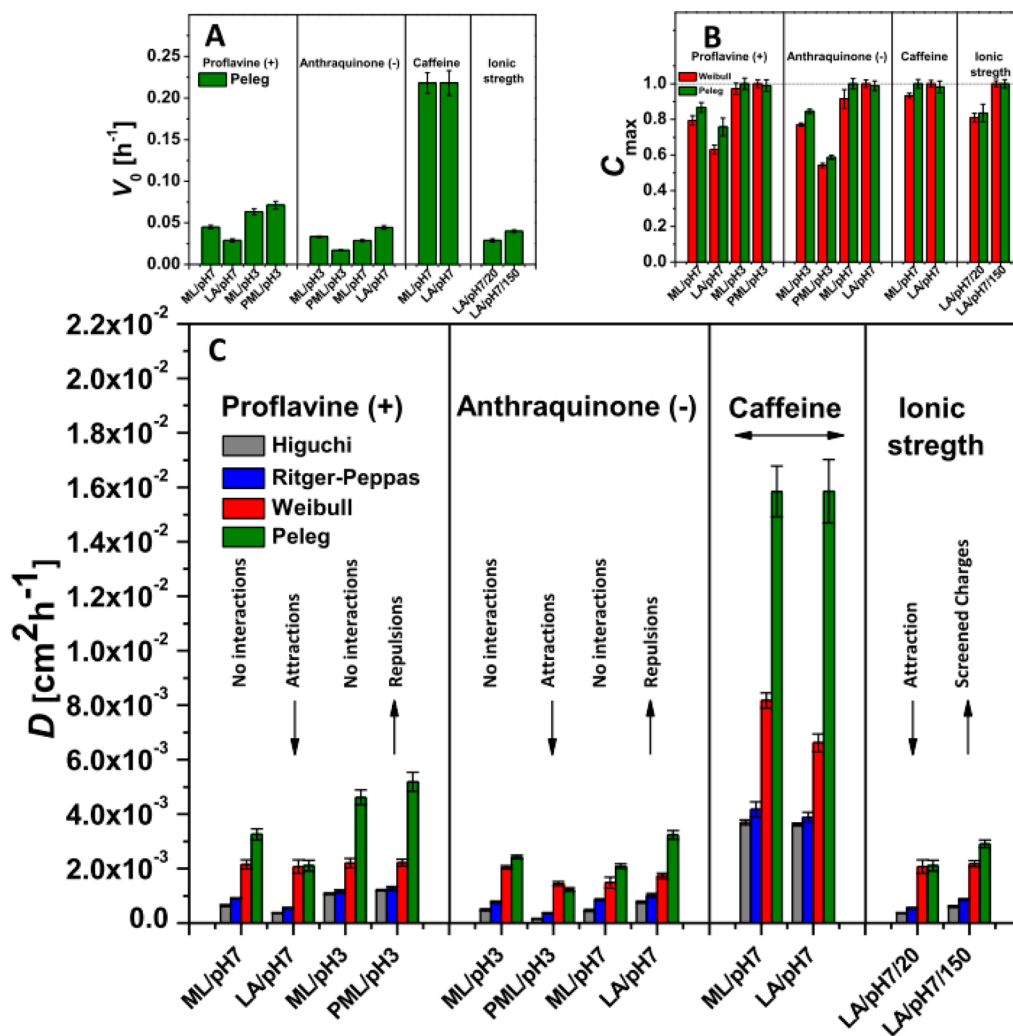


Figure 7. Comparison between the release parameters obtained from the different models: Higuchi (gray), Ritger–Peppas (blue), Weibull (red), and Peleg (green). (A) Initial velocity calculated from the Peleg model, (B) maximum released equilibrium concentration calculated from the Weibull and Peleg model, and (C) apparent diffusion coefficient from all models. Note: the maximum released concentration at equilibrium was normalized with respect to the maximum value of each drug obtained from release experiments.

1) and with the same initial speed V_0 of $22 \times 10^{-2} \text{ h}^{-1}$ in both cases.

Effect of the Ionic Strength. Release studies varying ionic strength were performed to further prove the effect of charge

interactions. To this end, the positive drug, proflavine (PF), was selected and release studies at pH 7 in LA doped systems were performed at either low ($I = 20$ mM) or high ionic strength ($I = 150$ mM) buffer conditions. These two values were selected

to be in two extreme cases of electrostatic interactions, as indicated by the corresponding Debye length, which was calculated in both cases ($I = 20$ and 150 mM) using the following equation for electrolytes:

$$k^{-1} = \sqrt{\frac{\epsilon_0 \cdot \epsilon_r \cdot k_B \cdot T}{2 \cdot N_A \cdot e^2 \cdot I}} \quad (9)$$

where ϵ_0 is the dielectric permittivity in vacuum ($\epsilon_0 = 8.85 \times 10^{-12}$ F m⁻¹), ϵ_r is the relative dielectric permittivity in water ($\epsilon_r = 80.1$), k_B is the Boltzmann's constant ($k_B = 1.38 \times 10^{-23}$ J K⁻¹), T is the absolute temperature (303 K), N_A is the Avogadro constant ($N_A = 6.02 \times 10^{23}$), e is the elementary electron charge ($e = 1.6 \times 10^{-19}$ C), and I is the total ionic strength (mol m⁻³). The values obtained were, respectively, $k^{-1}_{20} = 2.19$ nm at 20 mM buffer ionic strength and $k^{-1}_{150} = 0.8$ nm at 150 mM buffer ionic strength, thus respectively above and below the calculated radius of the LLCs water channels ($R_W = 1.97$ nm). Thus, it should be expected that at low ionic strength the charges of the drug and the hydrophilic head groups present on the surface of the water channels are able to interact, since the Debye length is larger than R_W , whereas at 150 mM being the Debye length smaller than R_W , the ions present in solution screen the charges, reducing the interactions between the drug and the mesophase channel walls. The data confirm indeed that release is triggered by the increase in the ionic strength (Figure 6).

Both the release rate and the diffusion coefficient at high ionic strength increased (Table 1). The values obtained for the system at high ionic strength were, respectively: 6.1×10^{-4} , 8.6×10^{-4} , 22×10^{-4} , and 29×10^{-4} cm² h⁻¹. This corresponds to an increase of 65%, 59%, 5%, and 38% for the system at high ionic strength compared to the one at low ionic strength. The initial velocity also featured an increase of 38%. The maximum release concentration obtained from the Peleg model confirmed that 16% of the drug was retained at low ionic strength while the release was complete at higher ionic strength.

To summarize, the pH responsiveness of the designed systems can be explained by considering the presence in the mesophase lipid bilayer, of a weak base (PML) or acid (LA), which induces a charge density variation in the water channel surfaces of the LLCs. These molecules can be protonated or deprotonated, depending on the pH, thus changing the surface charge density of the mesophase water channels and allowing for control in the release of charged drugs. Linoleic acid (LA) is negatively charged at pH 7; by decreasing the pH below the pK_a value of 5.5, the carboxylic group is mostly protonated, decreasing the surface charge density on the water channels at the water–lipid interface. Pyridinylmethyl linoleate (PML) acts exactly in the opposite way; the pyridinyl group ($pK_a = 5.4$) is positively charged at pH 3, while is deprotonated at higher pH values decreasing the surface charges and, therefore, the electrostatic interaction with the charged drugs. The unperturbed diffusion of neutral drugs and the “screening” effect of increasing ionic strength, further underline the importance of electrostatic interactions in these pH responsive mesophase systems. Figure 7 summarizes the initial velocity (Figure 7A), the maximum released concentration at the equilibrium (Figure 7B), and the apparent diffusion coefficient (Figure 7C) obtained from the different fitting models, giving an exhaustive overview of the phenomena described here.

The initial velocity, the inverse of the first Peleg constant k_1 , clearly shows that attractive drug–mesophase interactions led

to a decrease of the release velocity while repulsive interactions led to a slightly increase in the release rate. Further evidence for this process are given by the constant speed for the neutral drug, caffeine, and for the ionic strength-induced “screening” process, which increases the release velocity in the presence of attractive interactions (Figure 7A). The maximum concentration profile in Figure 7B also shows a decrease in the total amount of released drug when attractive interactions are active. The apparent diffusion coefficient (Figure 7C) follows similar trends. Overall, our findings show that is possible to design pH responsive bicontinuous cubic LLCs by doping the neutral monolinolein with both weak acids and bases. These doped systems are able to control the release of charged molecules at low ionic strength by tuning electrostatic interactions without the need of changing the liquid-crystalline structure.

CONCLUSIONS

Two new pH responsive monolinolein-based lyotropic liquid crystals have been designed by doping the original mesophase with either a weak acid, linoleic acid (LA), or a weak base, pyridinylmethyl linoleate (PML). These two systems are able to delay either the release of positively charged molecules at pH 7 or the release of negatively charged drugs at pH 3, respectively. At low ionic strength ($I = 20$ mM), release studies of drugs, may these be positively or negatively charged, from charged mesophases reveal the general trend that electrostatic attractions always lead to a slowing in the release behavior, while electrostatic repulsion does not significantly affect the release process, although a moderate acceleration can occasionally be observed. In contrast, neutral drugs diffuse independently of the presence and nature of charges present on the mesophase water channels surfaces. At high enough ionic strength, corresponding to Debye length of the buffer smaller than the radii of the mesophase water channels, charges are essentially screened, and release of charged drugs proceeds following a mechanism similar to that observed for the diffusion of neutral drugs. Four different models were considered to interpret comprehensively the electrostatic effects occurring during the release process, which allowed rationalizing further some experimental trends, such as the observed deviations from Fickian diffusion and specific drug–mesophase interactions.

ASSOCIATED CONTENT

Supporting Information

Pyridin-4-ylmethyl linoleate synthesis process and additional tables and other Supporting Information. This material is available free of charge via the Internet at <http://pubs.acs.org>.

AUTHOR INFORMATION

Corresponding Author

*E-mail: raffaele.mezzenga@hest.ethz.ch.

Notes

The authors declare no competing financial interest.

REFERENCES

- (1) Luzzati, V.; Husson, F. The structure of the liquid crystalline phases of lipid-water systems. *J. Cell Biol.* **1962**, *12*, 207–219.
- (2) Luzzati, V.; Tardieu, A.; Gulik-Krzywicki, T.; Rivas, E.; Reiss-Husson, F. Structure of the cubic phases of lipid-water systems. *Nature* **1968**, *220*, 485–488.
- (3) Scriven, L. E. Equilibrium bicontinuous structure. *Nature* **1976**, *263*, 123–125.

- (4) Mezzenga, R.; Schurtenberger, P.; Burbidge, P.; Michel, M. Understanding foods as soft materials. *Nat. Mater.* **2005**, *4*, 729–740.
- (5) Mezzenga, R.; Meyer, C.; Servais, C.; Romoscanu, A. I.; Sagalowicz, L.; Hayward, R. C. Shear Rheology of Lyotropic Liquid Crystals: A Case Study. *Langmuir* **2005**, *21*, 3322–3333.
- (6) Shah, J. C.; Sadhale, Y.; Chilukuri, D. M. Cubic phase gels as drug delivery systems. *Adv. Drug Delivery Rev.* **2001**, *47*, 229–250.C.
- (7) Guo, C.; Wang, J.; Cao, F.; Lee, R. J.; Zhai, G. Lyotropic liquid crystal systems in drug delivery. *Drug Discovery Today* **2010**, *15*, 1032–1040.
- (8) Fong, C.; Le, T.; Drummond, C. J. Lyotropic liquid crystal engineering—ordered nanostructured small molecule amphiphile self-assembly materials by design. *Chem. Soc. Rev.* **2012**, *41*, 1297–1322.
- (9) Seddon, A. M. In *Advances in planar lipid bilayers and liposomes*; Iglic, A., Kulkarni, C. V., Eds; Elsevier B.V.: Amsterdam, 2013; Vol. 18, pp 147–180.
- (10) Shah, J. C.; Sadhale, Y.; Chilukuri, D. M. Cubic phase gels as drug delivery systems. *Adv. Drug Delivery Rev.* **2001**, *47*, 229–250.
- (11) Boyd, B. J.; Whittaker, D. V.; Khoob, S. M.; Davey, G. Lyotropic liquid crystalline phases formed from glycerate surfactants as sustained release drug delivery systems. *Int. J. Pharm.* **2006**, *309*, 218–226.
- (12) Sagalowicz, L.; Leser, M. E.; Watzke, H. J.; Michel, M. Monoglyceride self-assembly structures as delivery vehicles. *Trends Food Sci. Technol.* **2006**, *17*, 204–214.
- (13) Sallam, A. S.; Khalil, E.; Ibrahim, H.; Freij, I. Formulation of an oral dosage form utilizing the properties of cubic liquid crystalline phases of glyceryl monooleate. *Eur. J. Pharm. Biopharm.* **2002**, *53*, 343–352.
- (14) Amar-Yuli, I.; Libster, D.; Aserin, A.; Garti, N. Solubilization of food bioactives within lyotropic liquid crystalline mesophases. *Curr. Opin. Colloid Interface Sci.* **2009**, *14*, 21–32.
- (15) Vallooran, J. J.; Negrini, R.; Mezzenga, R. Controlling Anisotropic Drug Diffusion in Lipid-Fe₃O₄ Nanoparticle Hybrid Mesophases by Magnetic Alignment. *Langmuir* **2013**, *29*, 999–1004.
- (16) Angelova, A.; Angelov, B.; Mutafchieva, R.; Lesieur, S.; Couvreur, P. Self-Assembled Multicompartment Liquid Crystalline Lipid Carriers for Protein, Peptide, and Nucleic Acid Drug Delivery. *Acc. Chem. Res.* **2011**, *44*, 147–156.
- (17) Fong, W. K.; Hanley, T. L.; Thierry, B.; Kirby, N.; Waddington, L. J.; Boyd, B. J. Controlling the Nanostructure of Gold Nanorod–Lyotropic LiquidCrystalline Hybrid Materials Using Near-Infrared Laser Irradiation. *Langmuir* **2012**, *28*, 14450–14460.
- (18) Garti, N.; Libster, D.; Aserin, A. Lipid polymorphism in lyotropic liquid crystals for triggered release of bioactives. *Food Funct.* **2012**, *3*, 700–713.
- (19) Fong, W. K.; Hanley, T.; Boyd, B. J. Stimuli responsive liquid crystals provide ‘on-demand’ drug delivery in vitro and in vivo. *J. Controlled Release* **2009**, *135*, 218–226.
- (20) Negrini, R.; Mezzenga, R. pH-responsive lyotropic liquid crystals for controlled drug delivery. *Langmuir* **2011**, *27*, 5296–5303.
- (21) Peng, S.; Guo, Q.; Hughes, T. C.; Hartley, P. G. Reversible Photorheological Lyotropic Liquid Crystals. *Langmuir* **2014**, *30*, 866–872.
- (22) Chang, C. M.; Bodmeier, R. Effect of dissolution media and additives on the drug release from cubic phase delivery systems. *J. Controlled Release* **1997**, *46*, 215–222.
- (23) Lindell, K.; Engblom, J.; Jonströmer, M.; Carlsson, A.; Engström, S. Influence of a charged phospholipid on the release pattern of timolol maleate from cubic liquid crystalline phases. *Prog. Colloid Polym. Sci.* **1998**, *108*, 111–118.
- (24) Clogston, J.; Caffrey, M. Controlling release from the lipidic cubic phase. Amino acids, peptides, proteins and nucleic acids. *J. Controlled Release* **2005**, *107*, 97–111.
- (25) Kwon, T. K.; Kim, J. C. Monoolein cubic phase containing acidic proteinoid: pH-dependent release. *Drug Dev. Ind. Pharm.* **2011**, *37*, 56–61.
- (26) Zabara, A.; Negrini, R.; Onaca-Fischer, O.; Mezzenga, R. Perforated Bicontinuous Cubic Phases with pH-Responsive Topological Channel Interconnectivity. *Small* **2013**, *9*, 3602–3609.
- (27) Nazaruk, E.; Szlêzak, M.; Gorecka, E.; Bilewicz, R.; Osornio, Y. M.; Uebelhart, P.; Landau, E. M. Design and Assembly of pH-Sensitive Lipidic Cubic Phase Matrices for Drug Release. *Langmuir* **2014**, *30*, 1383–1390.
- (28) Amar-Yuli, I.; Adamcik, J.; Blau, S.; Aserin, A.; Garti, N.; Mezzenga, R. Controlled embedment and release of DNA from lipidic reverse columnar hexagonal mesophases. *Soft Matter* **2011**, *7*, 8162–8168.
- (29) Ericsson, B.; Eriksson, P. O.; Loeffroth, J. E.; Engstroem, S.; Ferring, A. B.; Malmoe, S. Cubic phases as delivery systems for peptide drugs. *ACS Symp. Ser.* **1991**, *469*, 251–265.
- (30) Burrows, R.; Collett, J. H.; Attwood, D. Release of drugs from monoglyceride-water liquid crystalline phases. *Int. J. Pharm.* **1994**, *111*, 283–293A.
- (31) Higuchi, W. I. Diffusional Models Useful in Biopharmaceutics. *J. Pharm. Sci.* **1967**, *56*, 315–324.
- (32) Ritger, P. L.; Peppas, N. A. A simple equation for description of solute release. I. Fickian and non-Fickian release from non-swellaible devices in the form of slabs, spheres, cylinders or discs. *J. Controlled Release* **1987a**, *5*, 23–36.
- (33) Weibull, W. A Statistical Distribution Function of Wide Applicability. *J. Appl. Mech.* **1951**, *18*, 293–297.
- (34) Peleg, M. An Empirical Model for the Description of Moisture Sorption Curves. *J. Food Sci.* **1988**, *53*, 1216–1219.